Laboratory and Theoretical Study of the Oxy Radicals in the OH- and Cl-Initiated Oxidation of Ethene

John J. Orlando* and Geoffrey S. Tyndall*

Atmospheric Chemistry Division, National Center for Atmospheric Research, Boulder, Colorado 80303

Merete Bilde

Plant Biology and Biogeochemistry Department, Risø National Laboratory, DK-4000 Roskilde, Denmark

Corinne Ferronato

Groupe de Recherche sur l'Environnement et la Chimie Appliquée (GRECA), Université Joseph Fourier, F-38000 Grenoble, France

Timothy J. Wallington

Ford Research Laboratory, SRL-3083, Ford Motor Company, Dearborn, Michigan 48121-2053

Luc Vereecken and Jozef Peeters*

Department of Chemistry, University of Leuven, B-3001 Leuven, Belgium

Received: April 21, 1998; In Final Form: August 12, 1998

The products of the OH-initiated oxidation mechanism of ethene have been studied as a function of temperature (between 250 and 325 K) in an environmental chamber, using Fourier transform infrared spectroscopy for end product analysis. The oxidation proceeds via formation of a peroxy radical, $HOCH_2CH_2O_2$. Reaction of this peroxy radical with NO is exothermic and produces chemically activated $HOCH_2CH_2O$ radicals, of which about 25% decompose to CH_2OH and CH_2O on a time scale that is rapid compared to collisions, independent of temperature. The remainder of the $HOCH_2CH_2O$ radicals are thermalized and undergo competition between decomposition, $HOCH_2CH_2O \rightarrow CH_2OH + CH_2O$ (6), and reaction with O_2, $HOCH_2CH_2O + O_2 \rightarrow HOCH_2CHO + HO_2$ (7). The rate constant ratio, k_6/k_7, for the thermalized radicals was found to be $(2.0 \pm 0.2) \times 10^{25} \exp[-(4200 \pm 600)/T]$ molecule cm^{-3} over the temperature range 250−325 K. With the assumption of an activation energy of 1−2 kcal mol^{-1} for reaction 7, the barrier to decomposition of the $HOCH_2CH_2O$ radical is found to be 10−11 kcal mol^{-1}. A study of the Cl-atom-initiated oxidation of ethene was also carried out; the main product observed under conditions relevant to the atmosphere was chloroacetaldehyde, $ClCH_2CHO$. Theoretical studies of the thermal and "prompt" decomposition of the oxy radicals were based on a recent ab initio characterization that highlighted the role of intramolecular H bonding in $HOCH_2CH_2O$. Thermal decomposition is described by transition state and the Troe theories. To quantify the prompt decomposition of chemically activated nascent oxy radicals, the energy partitioning in the initially formed radicals was described by separate statistical ensemble theory, and the fraction of activated radicals dissociating before collisional stabilization was obtained by master equation analysis using RRKM theory. The barrier to $HOCH_2CH_2O$ decomposition is inferred independently as being 10−11 kcal mol^{-1}, by matching both of the theoretical $HOCH_2CH_2O$ decomposition rates at 298 K with the experimental results. The data are discussed in terms of the atmospheric fate of ethene.

Introduction

The oxidation of non-methane hydrocarbons (NMHCs) in the troposphere leads to the generation of ozone and other secondary pollutants such as peroxyacyl nitrates (PANs), other organic nitrates, and carbonyl species. Ethene is one of the more abundant NMHCs with a total source strength of about 18−45 Tg/yr.[1,2] Various natural sources of ethene to the atmosphere have been identified, including emissions from vegetation, soils, and the oceans. Ethene is also an important component of biomass burning and is produced in the consumption of fossil fuels.[1] The disparate nature of its sources, coupled with its short atmospheric lifetime (a day or two; see below), leads to a wide range of observed ethene mixing ratios (tens of parts per trillion over the oceans to tens of parts per billion in urban regions).[2−4] Despite its short lifetime, high concentrations of ethene are occasionally observed in the upper troposphere as the result of convection[4] or the lofting of biomass burning plumes.[5,6]

The oxidation of ethene in the atmosphere, as is the case for most hydrocarbons, is initiated predominantly by reaction with the OH radical.[7]

$$OH + C_2H_4 + M \rightarrow HOCH_2CH_2 + M \qquad (1)$$

S1089-5639(98)01937-9 CCC: $15.00
Published on Web 09/26/1998

The recommended value for the rate coefficient for reaction 1, $k_1 = 8.2 \times 10^{-12}$ cm^3 molecule^{-1} s^{-1}, at 1 atm total pressure and 298 K,[8] leads to an atmospheric lifetime for ethene of about 1−2 days. The hydroxyethyl radical rapidly adds O_2 to form a β-hydroxyalkylperoxy radical,[9,10] the subsequent reactions of which lead in large part to the generation of a β-hydroxyalkoxy radical, $HOCH_2CH_2O$.[10−14]

$$HOCH_2CH_2 + O_2 + M \rightarrow HOCH_2CH_2O_2 + M \quad (2)$$

$$HOCH_2CH_2O_2 + NO \rightarrow HOCH_2CH_2O + NO_2 \quad (3)$$

$$HOCH_2CH_2O_2 + RO_2 \rightarrow \text{products} \quad (4)$$

$$HOCH_2CH_2O_2 + HO_2 \rightarrow \text{products} \quad (5)$$

Oxy radicals such as $HOCH_2CH_2O$ can undergo two basic types of reaction, reaction with O_2 and decomposition via C−C bond rupture,[15,16] and it is this competition that determines which stable products are obtained in the oxidation process. Environmental chamber studies by Niki et al.[12,13] using FT-IR detection of end products revealed the formation of CH_2O and glycolaldehyde (hydroxyacetaldehyde, $HOCH_2CHO$) in the OH-initiated oxidation of ethene. These data were interpreted in terms of a competition between unimolecular decomposition of the oxy radical,

$$HOCH_2CH_2O + M \rightarrow CH_2OH + CH_2O + M \quad (6)$$

and its reaction with O_2,

$$HOCH_2CH_2O + O_2 \rightarrow HOCH_2CHO + HO_2 \quad (7)$$

A rate coefficient ratio $k_6/k_7 = 1.8 \times 10^{19}$ molecule cm^{-3} was reported for 1 atm total pressure at 298 K. The ratio is expected to be strongly temperature dependent, owing to the existence of an energy barrier to the occurrence of reaction 6, but no studies of the oxidation of ethene at $T < 298$ K have been reported to date.

The reactions of peroxy radicals with NO are in general exothermic by about 10−15 kcal mol^{-1}. Recent studies on halocarbon oxidation conducted in our laboratories[17−19] have shown that a significant fraction of this available energy is deposited into the internal modes of the oxy radical product, leading to an enhanced tendency for this radical to undergo unimolecular decomposition. This chemical activation is a result of the relatively long lifetime (>1 ps) of the peroxynitrite intermediate formed in the reaction of the peroxy radical with NO. Since the barrier to decomposition of the $HOCH_2CH_2O$ radical is expected to be only about 12−14 kcal mol^{-1},[16] such an effect may also be at work in the ethene system and may influence the observed products. To model the extent of prompt dissociation, one needs to know both the thermochemistry of the alkoxy radical decomposition reaction and the energy partitioning in the nascent products of the $RO_2 + NO$ reaction. To aid in the interpretation of the results, detailed calculations have been carried out to model the energy distribution in the products of reaction 3, the fraction of the activated oxy radicals that decomposes before undergoing collisions, and the rate of decomposition of thermalized oxy radicals.

The goals of this work were as follows: (1) to determine the products of the OH- and Cl-initiated oxidation of ethene over the temperature range encountered in the troposphere; (2) to investigate whether the extent to which chemical activation of the oxy radical occurs differs in the two reaction systems; (3) to interpret the results quantitatively using calculations of the decomposition rates of the oxy radicals from the separate statistical ensemble (SSE) theory. The relevance of the data to the atmospheric fate of ethene is discussed.

Experimental Section

The work described here was carried out in an environmental chamber, which has been described previously.[20,21] The apparatus consists of a 47 L stainless steel cell, 2 m in length, which is interfaced to a Fourier transform spectrometer (Bomem DA3.01) operating in the infrared spectral region. Multipass optics housed within the chamber provided a total path length of 32.6 m. Absorption spectra were obtained from the co-addition of 50−200 interferograms recorded at a resolution of 1 cm^{-1}. The temperature of the cell was controlled by flowing ethanol from a circulating bath (Neslab ULT-80DD) through a jacket surrounding the cell. The temperature in the chamber, as monitored using eight thermocouple gauges along its length, was found to be uniform along the length of the cell to within ±1 K. Photolysis was carried out using a Xe-arc lamp, the output of which was filtered with a Corning 7-54 filter to give radiation between 240 and 395 nm.

The OH-initiated oxidation of ethene was studied using the photolysis of mixtures of CH_3ONO (10−58 mTorr), C_2H_4 (125−360 mTorr), NO (9−90 mTorr), O_2 (70−700 Torr), and N_2 (0−630 Torr), at a total pressure of 700 Torr. For studies of the Cl-initiated oxidation, CH_3ONO was replaced in the mixture by Cl_2 (40−145 mTorr) and the O_2 pressure was varied between 2 and 700 Torr. The minor components of the gas mixtures were swept into the chamber from calibrated volumes using O_2 or N_2 carrier gas. Quantification of reactants and products in these experiments was achieved by comparison to standard spectra obtained in the environmental chambers at NCAR or at Ford Motor Company. The absorption feature used to quantify $HOCH_2CHO$ at 1107 cm^{-1} is strongly overlapped by that of HCOOH at 1105 cm^{-1}. Therefore, care was taken to ensure that the NO was not depleted, to avoid buildup of HCOOH from the reaction of HO_2 with CH_2O.

Hydroxyl radicals were generated in the cell from the CW photolysis of methyl nitrite (CH_3ONO) in the presence of added NO.

$$CH_3ONO + h\nu \rightarrow CH_3O + NO \quad (8)$$

$$CH_3O + O_2 \rightarrow CH_2O + HO_2 \quad (9)$$

$$HO_2 + NO \rightarrow OH + NO_2 \quad (10)$$

Methyl nitrite was prepared from the dropwise addition of sulfuric acid to a saturated solution of sodium nitrite in methanol[22] and degassed by multiple freeze−pump−thaw cycles prior to use. For most experiments at 298 K and all experiments at lower temperatures, $^{13}CH_3ONO$ was used so that formaldehyde formed from its photolysis could be differentiated spectroscopically from that formed in the ethene oxidation. Other gases were used as purchased, N_2 from the boil-off of a liquid N_2 Dewar, O_2 (UHP, U.S. Welding), Cl_2 (HP, Matheson), C_2H_4 (CP grade, Matheson), NO (Linde).

Experiments consisted of between two and five irradiations of a gas mixture, with an FTIR spectrum recorded after each irradiation. The overall conversion of ethene was always kept to less than 5% to avoid significant destruction of the products (formaldehyde, glycolaldehyde, and chloroacetaldehyde; see below), which have similar reactivities toward Cl and OH as ethene.[8,23−25]

Results and Discussion

OH-Initiated Oxidation of Ethene: Chemistry of the $HOCH_2CH_2O$ Radical. The peroxy radical $HOCH_2CH_2O_2$ was generated from the addition of OH to ethene via reactions 1 and 2. On the basis of our previous studies of HFC-134a and HFC-236cb oxidation,[17,18] the following mechanism can be used to describe the subsequent chemistry involving the formation of an excited oxy radical.

$$HOCH_2CH_2O_2 + NO \rightarrow HOCH_2CH_2O^* + NO_2 \quad (3)$$

$$HOCH_2CH_2O^* \rightarrow CH_2OH + CH_2O \quad (11)$$

$$HOCH_2CH_2O^* + M \rightarrow HOCH_2CH_2O + M \quad (12)$$

$$HOCH_2CH_2O + M \rightarrow CH_2OH + CH_2O + M \quad (6)$$

$$HOCH_2CH_2O + O_2 \rightarrow HOCH_2CHO + HO_2 \quad (7)$$

$$CH_2OH + O_2 \rightarrow CH_2O + HO_2 \quad (13)$$

In this analysis, any oxy radicals that are produced above the barrier to decomposition are assumed to decompose rapidly on a time scale that is short relative to collisions, as represented by reaction 11. Radicals that are produced below the decomposition barrier suffer numerous collisions and are thus thermalized (reaction 12) before undergoing decomposition (reaction 6) or reaction with O_2 (reaction 7). If we use the quantity α to represent the yield of thermalized radicals, then the yield of glycolaldehyde (Y_{GA}) is given as follows:

$$Y_{GA} = \alpha\{k_7[O_2]/(k_7[O_2] + k_6)\} \quad (A)$$

and

$$[Y_{GA}]^{-1} = (1/\alpha)\,[k_6/k_7[O_2] + 1] \quad (B)$$

Because small conversions of ethene were employed in these experiments, yields of glycolaldehyde were not obtained relative to the amount of ethene consumed but instead were obtained from a consideration of the relative yields of glycolaldehyde and formaldehyde. In this case, since two molecules of formaldehyde are formed,[13]

$$Y_{GA} = [HOCH_2CHO]/\{0.5[CH_2O] + [HOCH_2CHO]\} \quad (C)$$

From (B) above, it is clear that values of α and k_6/k_7 can be obtained from a plot of the inverse of the glycolaldehyde yield versus the inverse O_2 pressure, provided no other losses of the thermalized oxy radicals occur. A plot of this type (for 700 Torr total pressure and 298 K) is shown in Figure 1. The data shown include those obtained using $^{13}CH_3ONO$ as the OH radical source as well as some initial data obtained using $^{12}CH_3ONO$. Product yield data obtained using $^{12}CH_3ONO$ had to be corrected for production of $^{12}CH_2O$ from the decomposition of $^{12}CH_3ONO$, reactions 8 and 9:

$$[^{12}CH_2O]_{t,corr} = [^{12}CH_2O]_{t,obs} - \{[^{12}CH_3ONO]_o - [^{12}CH_3ONO]_t\}$$

where $[^{12}CH_2O]_{t,corr}$ and $[^{12}CH_2O]_{t,obs}$ are the corrected and observed formaldehyde concentrations at time t and $[^{12}CH_3ONO]_o$ and $[^{12}CH_3ONO]_t$ are the initial concentration of methyl nitrite and its concentration at time t. A least-squares fit of the data shown in Figure 1 yields an intercept of 1.35 ± 0.15 and a slope of 540 ± 80 Torr, from which values of $\alpha = 0.74 \pm 0.10$ and $k_6/k_7 = (1.32 \pm 0.20) \times 10^{19}$ molecule cm^{-3} can be obtained (all uncertainties are 2σ). Also shown in Figure 1 (but not included in the fit) are data reported by Niki et al.[13] under the same conditions of pressure and temperature. As will be further discussed below, these data are clearly consistent with our data and are also indicative of a nonunity intercept in the $1/Y_{GA}$ vs $1/[O_2]$ plot.

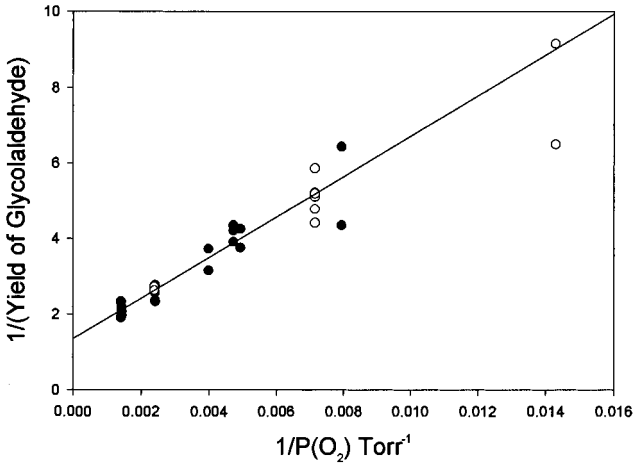

Figure 1. Plot of the inverse yield of glycolaldehyde versus the inverse oxygen pressure, from the OH-initiated oxidation of ethene at 700 Torr total pressure. Data shown are for 298 K: filled circles, this work; open circles, Niki et al.[13]

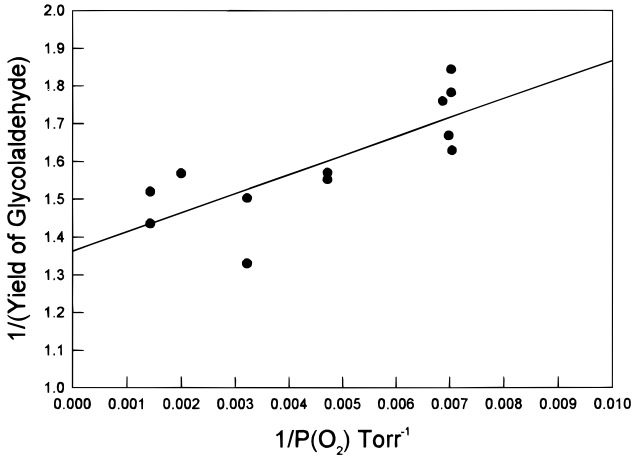

Figure 2. Plot of the inverse yield of glycolaldehyde versus the inverse oxygen pressure, from the OH-initiated oxidation of ethene at 250 K and 700 Torr total pressure. The data have been corrected for loss of $HOCH_2CH_2O$ radicals by reaction with NO or NO_2 as described in eq E.

The nonunity intercept obtained in Figure 1 is a strong indication of the occurrence of prompt decomposition (reaction 11) of a significant fraction of the oxy radicals formed in reaction 3. However, the value of α, and hence the magnitude of the hot alkoxy radical effect, obtained from Figure 1 is quite uncertain, owing to a fairly substantial extrapolation. The best demonstration of the occurrence of prompt decomposition of the oxy radicals produced in reaction 3 is obtained at low temperature and high O_2 pressures. Under these conditions, most thermalized radicals should react with O_2 (owing to the strong temperature dependence anticipated for reaction 6) and significant yields of formaldehyde must originate from prompt decomposition of chemically activated oxy radicals. Data for the lowest temperature studied, 250 K, are shown in Figure 2. Clearly, even at 250 K and 700 Torr of O_2, there is a significant

yield of formaldehyde and only about a 70% yield of glycolaldehyde. As the amount of O_2 is decreased, the glycolaldehyde yield does decrease, but only slightly, owing to a small amount of decomposition of the thermalized oxy radicals (reaction 6). At cold temperatures, the possibility exists that the thermalized oxy radicals react with NO or NO_2 in addition to reactions 6 and 7.

$$HOCH_2CH_2O + NO\ (NO_2) \rightarrow HOCH_2CH_2{-}ONO\ (-ONO_2) \quad (14)$$

In this case, eq A can be modified to take account of the loss of radicals, assuming similar rate coefficients for the reactions of NO and NO_2 with $HOCH_2CH_2O$.

$$Y_{GA} = \alpha\{k_7[O_2]/(k_7[O_2] + k_6 + k_{14}[NO_x])\} \quad (D)$$

The apparent glycolaldehyde yield, relative to the sum $\{0.5[CH_2O] + [HOCH_2CHO]\}$, can then easily be shown to be given by eq E.

$$Y_{APP} = \alpha\{k_7[O_2]/(k_7[O_2] + k_6 + (1 - \alpha)k_{14}[NO_x])\} \quad (E)$$

Some experiments were performed using elevated levels of NO at 250 and 255 K to look for a reduction in the yield of glycolaldehyde associated with the formation of hydroxynitrites or nitrates. A small change in the glycolaldehyde yield was observed (about 10%) when the ratio $[NO]/[O_2]$ was increased to 3000. Analytical fits to the observed data using eq E showed that the ratio k_{14}/k_7 is probably in the range 3000−4000. The data were thus corrected for loss of the thermalized oxy radicals using $k_{14}/k_7 = 3000$ with values for α and k_6/k_7 estimated from the experiments at higher temperatures. A plot of $1/Y_{GA}$ versus $1/[O_2]$ for the corrected data is shown in Figure 2 and yields a ratio $k_6/k_7 = (1.7 \pm 0.5) \times 10^{18}$ molecule cm^{-3} and a yield of stabilized radicals, α, of 0.71 ± 0.10. The reactions of alkoxy radicals with NO and NO_2 are normally at the high-pressure limit at 700 Torr, with rate coefficients of the order $(2-4) \times 10^{-11}$ cm^3 molecule^{-1} s^{-1}.[16,26] Thus, the reaction of $HOCH_2CH_2O$ with O_2 is of the order $(6-8) \times 10^{-15}$ cm^3 molecule^{-1} s^{-1} at 250 K, similar to the reaction of ethoxy radicals with O_2.[16,26]

Data were obtained at intermediate temperatures as well (Figure 3). In all cases, a nonunity intercept in the $1/Y_{GA}$ vs $1/[O_2]$ plot was obtained, with an average value at all temperatures studied of 1.34 ± 0.10. Since there was no significant variation of the intercept with temperature, we report a temperature-independent yield of thermalized oxy radicals of 0.75 ± 0.06. Values of the rate coefficient ratio k_6/k_7 were also obtained at each temperature studied. The slopes and intercepts at each temperature are summarized in Table 1. The slopes of the plots typically had uncertainties of 20%. The data at 256 K were corrected for the loss of RO radicals using eq E. Above 256 K, decomposition of the oxy radical is sufficiently rapid that the NO_x reactions do not have a major effect on the yields, and no correction was made. The data are plotted in Arrhenius form in Figure 4.

Product yield experiments were also carried out at 315 and 325 K. Because of the small yields of glycolaldehyde at these temperatures (due to rapid decomposition of $HOCH_2CH_2O$), experiments were only conducted at 700 Torr of O_2. Measured yields of glycolaldehyde under these conditions were $27 \pm 4\%$ (315 K) and $19 \pm 3\%$ (325 K). While accurate values of k_6/k_7 cannot be obtained in the absence of a full O_2 dependence of the product yields, a rough estimate can be obtained by constructing a plot of $1/Y_{GA}$ versus $1/[O_2]$ using an assumed intercept of 1.34 (the average value determined above) and the single data point at 700 Torr. Values of k_6/k_7 obtained in this fashion (also shown in Figure 4) have been assigned an uncertainty of $\pm 30\%$.

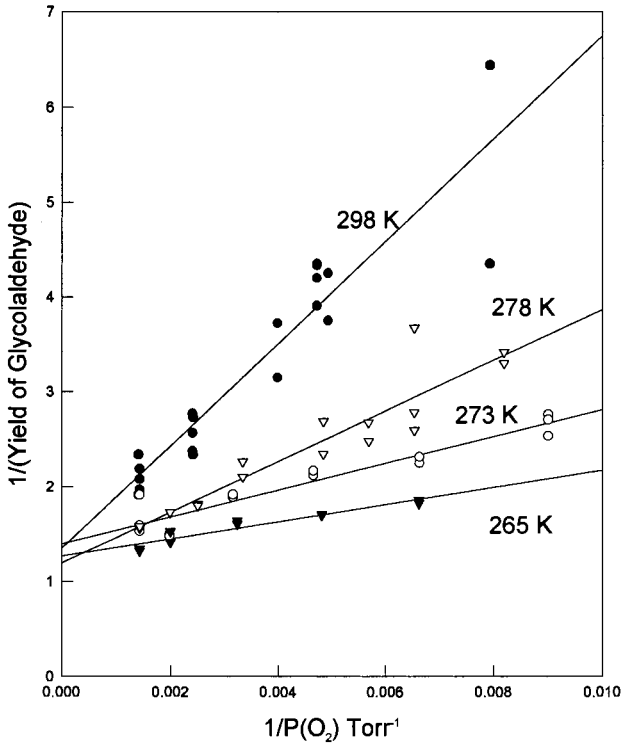

Figure 3. Plot of the inverse yield of glycolaldehyde versus the inverse oxygen pressure, from the OH-initiated oxidation of ethene at 700 Torr total pressure. Data shown are for 298 K (●), 278 K (▽), 273 K (○), and 265 K (▼).

TABLE 1: Summary of Dissociation Rate Coefficients at 700 Torr and Fraction of Stabilized Oxy Radicals Measured in This Study[a]

temp K	k_6/k_7 10^{18} molecule cm^{-3}	k_6 s^{-1}	α
325	64 ± 21	8.0×10^5	
315	39 ± 13	4.5×10^5	
298	13 ± 2	1.3×10^5	0.74 ± 0.10
278	6.4 ± 1.6	5.3×10^4	0.83 ± 0.15
273	3.7 ± 0.8	2.9×10^4	0.71 ± 0.09
265	2.5 ± 0.5	1.9×10^4	0.79 ± 0.08
256	1.5 ± 0.5	1.0×10^4	0.82 ± 0.10
250	1.7 ± 0.5	1.1×10^4	0.71 ± 0.10

[a] k_6 was calculated using $k_7 = 6 \times 10^{-14} \exp(-550/T)$ cm^3 molecule^{-1} s^{-1}, the same as for $C_2H_5O + O_2$.[8,26]

A linear least-squares fit to all the data shown in Figure 4 yields $k_6/k_7 = (2.0 \pm 0.2) \times 10^{25} \exp[-(4200 \pm 600)/T]$ molecule cm^{-3}, where the error in the pre-exponential factor reflects the uncertainty in the room-temperature value. Because of the large uncertainty in the values obtained at 250 and 256 K (due to a very small variation in the glycolaldehyde with O_2 pressure), these points were given a weight of 0.5 in the fit, as were the single-point determinations at 315 and 325 K. If an activation energy of 1−2 kcal mol^{-1} is assumed for the reaction of $HOCH_2CH_2O$ with O_2, as is the case for the analogous reactions of CH_3O and CH_3CH_2O,[8] then an Arrhenius activation energy of 9.5−10.5 kcal mol^{-1} is obtained for the decomposition of $HOCH_2CH_2O$, reaction 6, at 700 Torr. As discussed below, the reaction is expected to be in its falloff regime such that the corresponding barrier height E_b can be estimated at 10−11 kcal

mol^{-1}. The values for k_6 given in Table 1 have been calculated using a rate coefficient of $6 \times 10^{-14} \exp(-550/T)$ cm^3 molecule^{-1} s^{-1} for the reaction with O_2, which is the same as that for $C_2H_5O + O_2$.[8,26] While considerable uncertainty exists in any individual determination of α and k_6/k_7, the theoretical treatment presented later shows that chemical activation is expected for the barrier to decomposition measured here; thus, we are justified in analyzing the data in this way.

Our data can be compared with previous room-temperature studies of the OH-initiated oxidation of ethene. The product yield data of Niki et al.[13] at room temperature are in very good agreement with our work (see Figure 1). However, the earlier study did not account for the occurrence of prompt decomposition of the $HOCH_2CH_2O^*$ radical. Therefore, despite the observation of indistinguishable product yields, Niki's value of $k_6/k_7 = 1.8 \times 10^{19}$ molecule cm^{-3} at 298 K and 1 atm total pressure differs from ours.

Barnes et al.[14] also conducted chamber studies of the OH-initiated oxidation of ethene. Their data show an increased yield of formaldehyde versus glycolaldehyde when NO was added to their system, consistent with the occurrence of prompt decomposition of the $HOCH_2CH_2O$ radical in the presence of NO. In the absence of NO, the product studies are complicated by the presence of hydroperoxides and ethene glycol from the self-reaction, which are very difficult to calibrate. However, the variation of the yields of formaldehyde and glycolaldehyde measured by Barnes et al. as a function of O_2 pressure is consistent with the present results.

Cl-Initiated Oxidation of Ethene: Chemistry of the $ClCH_2CH_2O$ Radical. A study of the Cl-initiated oxidation of ethene was also carried out, using photolysis of Cl_2 as the source of Cl atoms. Initial experiments were conducted in the absence of NO such that the major fate of the $ClCH_2CH_2O_2$ radical was the self-reaction 17.[25,27]

$$Cl + C_2H_4 + M \rightarrow ClCH_2CH_2 + M \quad (15)$$

$$ClCH_2CH_2 + O_2 + M \rightarrow ClCH_2CH_2O_2 + M \quad (16)$$

$$2ClCH_2CH_2O_2 \rightarrow 2ClCH_2CH_2O + O_2 \quad (17a)$$

$$\rightarrow ClCH_2CHO + ClCH_2CH_2OH + O_2 \quad (17b)$$

$$ClCH_2CH_2O \rightarrow CH_2Cl + CH_2O \quad (18)$$

$$ClCH_2CH_2O + O_2 \rightarrow ClCH_2CHO + HO_2 \quad (19)$$

$$ClCH_2CH_2O_2 + HO_2 \rightarrow ClCH_2CH_2OOH + O_2 \quad (20)$$

Significantly different branching ratios $k_{17a}/(k_{17a} + k_{17b})$ have been reported, 0.69 ± 0.02 by Wallington et al.[27] and 0.57 ± 0.02 by Yarwood et al.[25] The CH_2Cl radical, if formed, would be converted predominantly to HCOCl in air and to both CO and HCOCl at low O_2.[28,29]

Products observed in our system in 700 Torr of synthetic air were chloroacetaldehyde, $ClCH_2CHO$ (molar yield of 86%), $ClCH_2CH_2OH$ (yield of 16%), and HCOCl (yield of 3%). The hydroperoxide product of reaction 20 was not observed in our system, although modeling studies using the Acuchem program[30] with published rate coefficient data[31] for reactions 17 and 20 indicate that its yield should be about 35%. The excellent mass balance observed in our experiments leads us to the conclusion that the hydroperoxide is converted to $ClCH_2CHO$ and H_2O on the chamber surfaces, similar to the behavior of other peroxides

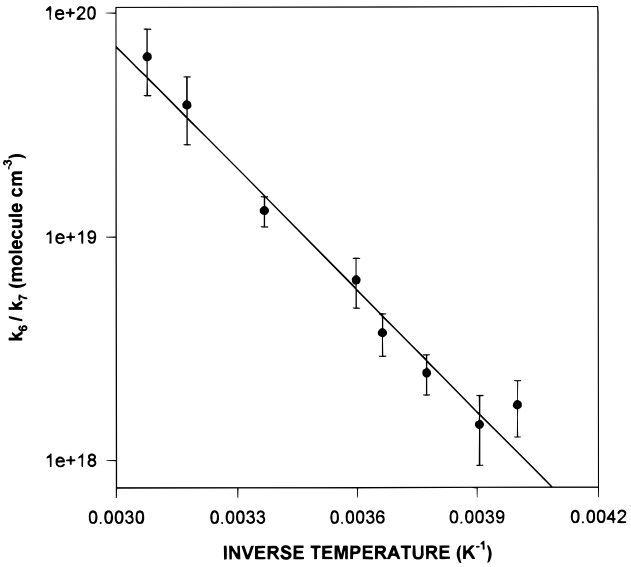

Figure 4. Arrhenius plot showing the logarithm of the rate constant ratio k_6/k_7 as a function of inverse temperature. Solid line is a least-squares fit to the data.

in our system.[32] The observed product yields can be used to derive a branching ratio, $k_{17a}/(k_{17a} + k_{17b}) = 0.55$, in good agreement with the data of Yarwood et al.[25]

The large yield of $ClCH_2CHO$ and the absence of CH_2O in the Cl-atom-initiated oxidation of ethene in air clearly indicate the predominance of reaction 19 over reaction 18 under these conditions, consistent with previous studies.[25,27] An analogous mechanism for the formation of $BrCH_2CHO$ from the reaction of Br with ethene has also been reported.[25,33] Only at very low O_2 concentrations (2−10 Torr) was any formaldehyde observed in our experiments; these data were consistent with a rate coefficient ratio of $k_{18}/k_{19} = (6 \pm 3) \times 10^{15}$ molecule cm^{-3}.

Further experiments were carried out in 700 Torr of air with added NO (10−80 mTorr) to look for evidence of chemical activation of the oxy radical. Complications arise in this system due to the generation of OH via reaction 19 followed by reaction 10. The subsequent reaction of OH with ethene then leads to production of CH_2O, which makes unambiguous identification of reaction 18 difficult. While $ClCH_2CHO$ and CH_2O were found in almost comparable yields, no HCOCl was observed. Simulations of the experiments using a chemical box model of the system showed that the observed formaldehyde could all be attributed to OH-initiated chemistry and that very little (if any) decomposition of the $ClCH_2CH_2O$ radical was occurring. Thus, even with NO present, $ClCH_2CHO$ is again the dominant product formed in the Cl-initiated oxidation of ethene, and no significant chemical activation effect is observed, in contrast to the OH-initiated oxidation.

Theoretical Prediction of Prompt Decomposition. Reactions of alkylperoxy radicals with NO, forming alkoxy radicals and NO_2, are exoergic by some 10−15 kcal mol^{-1}; moreover, the reactants can possess significant amounts of thermal internal energy. Since these processes occur via an intermediate combination product, a peroxynitrite, much of the excess energy should end up as vibrational energy of the largest product, the oxy radical. The term "vibrational" includes here the internal rotations. The nascent vibrational energy distribution of the oxy radical, $P(E_v)$, together with the energy-specific rates of the competing unimolecular dissociation and collisional stabilization processes, will determine the fraction of oxy radicals that decompose promptly, $(1 - \alpha)$. If the lifetime τ of the

activated intermediate is sufficiently long for random partitioning of its internal energy over all its vibrational degrees of freedom, the $P(E_v)$ distribution will also be governed by statistics and hence can be predicted with an adequate theory. Generally, the ergodicity condition is met for $\tau \geq 10^{-12}$ s. By adoption of relative energies for the reactants, the peroxynitrite intermediate and the products of reaction 3, as for the 1-butyl analogue,[34] one finds an $HOCH_2CH_2OONO^*$ RRKM lifetime $\tau \approx 5 \times 10^{-12}$ s, which meets the ergodicity criterion; at the same time, τ is short enough to be able to neglect collisional energy loss of the ROONO* under atmospheric conditions. The dissociation of peroxynitrites into RO + NO_2 occurs on a "type II" potential energy surface (PES) without a PE maximum in the exit channel,[34] implying a loose and late transition state (TS). Nitrate formation from the short-lived activated peroxynitrite cannot compete with the very fast prompt dissociation because the far more rigid ROONO → $RONO_2$ transition state is entropically at a disadvantage.

The separate statistical ensemble (SSE) theory for statistical partitioning of the available energy over the various degrees of freedom (d.f.) of the dissociation products of a vibrationally activated parent was developed by Wittig et al.[35] specifically for dissociation on a type II PES via a loose TS. Of course, ergodicity is the primary condition. The SSE theory is a refined version of phase space theory. SSE recognizes explicitly that the vibrational energies of the fragments of a dissociation process are determined solely by the "hot" vibrations of the activated parent. When a molecule with n vibrational modes dissociates into two fragments, with n_1' and n_2' vibrational modes, respectively, the remaining modes evolve into the $r = n - (n_1' + n_2')$ d.f. of relative translation/rotation motion of the fragments. For a type II PES, the energy E_d available for distribution over the above three sets of product d.f. is equal to the vibrational energy in all n modes of the parent, E_a, less the dissociation barrier E_o. Wittig et al.[35] have shown that, for a loose, productlike TS, a statistical distribution of E_d over all n internal d.f. of the dissociating molecule amounts to equal probabilities for all product quantum states with total energy E_d. Therefore, the distribution of E_d over the three sets of d.f. involved, the n_1' and n_2' vibrations of fragments 1 and 2, respectively, and the r d.f. of relative motion, will be determined uniquely by the combined densities of quantum states for each of these sets or, more precisely, by the energy dependences thereof. The r modes of relative motion are treated as unhindered free particle d.f., with combined state density therefore varying as $E^{((r/2)-1)}$. SSE has been validated for a number of photodissociation processes.[35,36] It must be stressed that the basic tenet of the SSE theory, i.e., that there is no free flow of energy between the d.f. of overall rotation of a molecule and its internal modes and that therefore only the internal energy of the parent will determine the internal energy distribution of the separating fragments, is not dependent on the way the activated molecule is prepared, be it by photoexcitation or otherwise.

To implement SSE theory for the products of reaction 3, the vibrational state densities of the products RO and NO_2 were calculated by exact counts.[37] The $HOCH_2CH_2O$ frequencies were taken from a theoretical B3LYP-DFT/6-31G** study.[38] This study identified several internal rotation conformers. The lowest-lying, "cis−cis", with the two O atoms nearly in a cis arrangement (dihedral angle ±50°, two enantiomers), is stabilized by intramolecular hydrogen bonding between the hydroxyl H and the oxy O. The other rotamers, denoted as "trans", have the two O atoms in a trans arrangement and/or the hydroxyl H in a trans position with respect to the oxy carbon; the lowest of these ("trans−trans") lies 1.9 kcal mol^{-1} above the cis−cis (all relative energies include zero-point vibration energy differences). In implementing SSE, the vibration manifolds of all rotamers were folded together; this amounts to assuming that discrete vibrational states of different rotamers can arise in reaction 3 with an equal probability, confined by the energy, entirely in keeping with the basic SSE philosophy. The final $P(E_v)$ function for the RO resulting from the thermal reaction 3 must be obtained by integration over the distribution of the E_d energies. For this reaction without barriers in the entrance or exit channels,[34] the internal energy available to the products, E_d, is equal to the reaction exoergicity, $-\Delta E_r(3)$, plus the internal thermal energy of the (variational) entrance transition state, E_{th}, which derives from the thermal energy of the reactants and which therefore shows a distribution. For ΔE_r, the value of −11 kcal mol^{-1} for the analogous $CH_3CH_2O_2$ reaction[26] was adopted (an H bridge as in $HOCH_2CH_2O$ is also found for $HOCH_2CH_2O_2$, appearing to be only slightly stronger[38]). The E_{th} distribution of the entrance TS was obtained from the sum of states function $G^{\ddagger}(E)\exp(-E/kT)$,[39] using approximate frequencies.[38] The average value of $\langle E_{th} \rangle$ at 298 K is 4 kcal mol^{-1}. As the peroxynitrite suffers no collisions during its lifetime, the rotational energy of the exit transition state may differ from the $E(\text{rot}) = (3/2)kT$ value[39] for the entrance transition state, in accordance with the corresponding moments of inertia. However, both transition states are variational and similarly loose such that the rotational energy change should be at most $\sim kT$; the correspondingly small effect (<0.6 kcal^{-1} mol^{-1}) on the available internal energy E_d was not taken into account. The resulting nascent $P(E_v)$ distribution function calculated for $HOCH_2CH_2O$ formed in reaction 3 at 298 K is shown in Figure 5. The average energy is 9.5 kcal mol^{-1}, i.e., below the "equipartition" value of 10.5 kcal mol^{-1}; the fwhm width of the distribution is almost 8 kcal mol^{-1}.

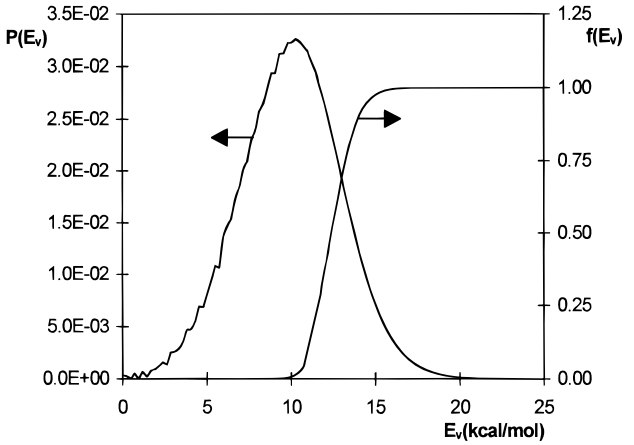

Figure 5. Predicted nascent vibrational energy distribution $P(E_v)$ of the $HOCH_2CH_2O$ radical formed in reaction 3 at 298 K; energy grain size = 0.239 kcal mol^{-1}. Predicted probability $f(E_v)$ of prompt dissociation at 760 Torr N_2 for $E_b(6) = 11$ kcal mol^{-1}.

Of the activated oxy radicals with internal energy E_v higher than the dissociation barrier $E_b(6)$, a fraction $f(E_v)$ will decompose promptly, in competition with collisional stabilization. Since the energy-specific unimolecular dissociation rate constant $k(E_v)$ increases rapidly with E_v, the fraction $f(E_v)$ tends to unity for large E_v. The $f(E_v)$ and the overall fraction of oxy radicals decomposing promptly, $(1 - \alpha)$, which are both pressure dependent, were obtained by master equation analysis of the combined unimolecular dissociation/collisional energy transfer system, with $P(E_v)$ as input. As master equation code we used

our recently developed fast and rigorous direct calculation of product distribution method,[40] which was inspired by the exact stochastic method of Gillespie.[41] The $k(E_v)$ are calculated according to RRKM theory, based on the (scaled) B3LYP-DFT vibration frequencies.[38] Densities and sums of states needed for the $k(E_v)$ are obtained by exact counts. Collisional energy-transfer probabilities were calculated according to the biexponential Troe model, adopting an average energy transfer per $RO-N_2$ collision, $\langle\Delta E\rangle$, of -100 cm^{-1} [42] and obeying detailed balance.

The critical parameter here is the energy barrier for the decomposition of $HOCH_2CH_2O$ to $CH_2OH + CH_2O$, $E_b(6)$. There are four ways to estimate this barrier. First, from the experimental data, an Arrhenius activation energy of about 10 kcal mol^{-1} was derived for the thermal dissociation at 700 Torr. Second, the modified Evans−Polanyi correlation relating the activation barrier E_b to the ionization potential IP and the endothermicity ΔH_d recently proposed by Atkinson[16] and shown in eq F suggests an activation energy of 12.5−14.5 kcal mol^{-1}, depending on the adopted heat of dissociation.

$$E_b = (2.4(\mathrm{IP}) - 8.1) + 0.36\Delta H_d \qquad \text{(F)}$$

Third, the above-mentioned B3LYP-DFT study[38] identified a "cis−cis TS", with the hydroxyl H and oxy O still interacting, at 9.9 kcal mol $^{-1}$ above the cis−cis oxy zero-point level and also a set of "trans TS" rotamers an additional 1.9−3.2 kcal mol^{-1} higher; note that the probable error on E_b for this level of theory is 3 kcal mol^{-1}.[43] Finally, E_b can be estimated from the experimental ratio $k_6/k_7 = 1.3 \times 10^{19}$ molecule cm^{-3} at 298 K and 700 Torr. Given that the known k_7 values at 298 K for small C_2 and C_3 oxy radicals are all close to 1×10^{-14} cm^3 molecule^{-1} s^{-1},[26] one can expect a similar value here. A k_7 value close to 10^{-14} is indeed supported by the NO addition experiments. In this way, one can estimate the thermal rate coefficient k_6 at 1.3×10^5 s^{-1} at 298 K, with an expected error of less than a factor of 4. In the thermal dissociation, only the lower-energy cis−cis rotamers of the oxy radical and of the transition state are of importance. Using the B3LYP-DFT vibration frequencies and moments of inertia,[38] the pre-exponential factor of the TS theory high-pressure rate coefficient was calculated; $(k_B T/h)(Q^{\ddagger}/Q) = 1.1 \times 10^{13}$ s^{-1} at 298 K. On the basis of the Troe low-pressure nonequilibrium theory[44] and the Troe falloff formalism,[45] it was found that the thermal rate constant k_6 at 700 Torr and 298 K is still almost 3 times lower than its high-pressure limit. Hence, one derives $E_b(6) = 10.2$ kcal mol^{-1}, with a possible error of ±0.8 kcal mol $^{-1}$. This value agrees very well with the experimental T dependence of k_6/k_7. We therefore conclude that the barrier is in the 10−11 kcal mol^{-1} range.

The fraction of $HOCH_2CH_2O^*$ radicals decomposing promptly was calculated for E_b values of 10 and 11 kcal mol^{-1}. In the master equation analysis, the (fast) interconversion of the activated cis−cis and trans rotamers was incorporated, together with their decomposition via the cis−cis TS and the trans TS's. Our master equation codes[40] allow for several different activated species simultaneously, each involved in a large number of parallel and competing unimolecular reactions and collisional energy-transfer processes. The results, for 298 K and 760 Torr of N_2 total pressure, can be summarized in terms of the overall fraction $(1 - \alpha)$. For an E_b value (i.e., the relative energy of the cis−cis TS with respect to the cis−cis radical ground state) of 10 kcal mol^{-1}, we calculated 38% prompt dissociation, whereas for $E_b = 11$, we obtained 21.5%. An E_b value of 13 kcal mol^{-1} results in only 4.8% dissociation. These data demonstrate the sensitivity of the theoretical predictions to the choice of E_b; moreover, considering that the experimental value of $(1 - \alpha)$ is 25%, the calculated results endorse an E_b in the 10−11 kcal mol^{-1} range. The theoretical result is also sensitive to the value of the exoergicity of the $RO_2 + NO$ reaction, $-\Delta E_r(3)$. Increasing it from 11 to 13 kcal mol^{-1}, for $E_b = 11$ kcal mol^{-1}, entails an increase of $(1 - \alpha)$ from 21.5 to 40%. On the other hand, the calculated values are only moderately sensitive to the relative stability of the two types of rotamers and to the vibrational parameters. Figure 5 shows the energy-specific dissociation probability $f(E_v)$ for $E_b = 11$ kcal mol^{-1}. The small low-energy tail, below the 11 kcal mol^{-1} barrier, is due to collisional activation effects. There will of course be a pressure effect on the rate of rise of the $f(E_v)$ curve and hence also on $(1 - \alpha)$; for total pressures of 380, 760, and 1520 Torr of N_2, the calculated $(1 - \alpha)$ values for $E_b = 11$ kcal mol^{-1} are 26.1, 21.5, and 16.9%, respectively. However, such small changes would be difficult to distinguish in the present experiments.

Finally, it should be noted that the rate coefficient for the thermal decomposition of $HOCH_2CH_2O$ given by Atkinson,[16] 4.6×10^3 s^{-1} at 298 K, is much smaller than that measured here, despite the lower pre-exponential factor deduced in this work. This is a result of the much larger activation energy used by Atkinson (14.5 kcal mol^{-1}). Additionally, the present calculations suggest that the thermal decomposition rate coefficient is still a factor of 3 from the high-pressure limit at 700 Torr, a conclusion that awaits experimental confirmation.

The prompt dissociation of $ClCH_2CH_2O$ formed in the $ClCH_2CH_2O_2 + NO$ reaction is more difficult to quantify theoretically because experimental data on the barrier to decomposition, $E_b(18)$, are lacking. Assuming that the difference between the heats of formation (at 298 K) of $ClCH_2CH_2O$ and CH_3CH_2O is equal to that between C_2H_5Cl and C_2H_6, the heat of dissociation of $ClCH_2CH_2O$ can be estimated from known data[26,46] as 14 kcal mol $^{-1}$. The corresponding E_b predicted by the recent Atkinson correlation[16] is 17.5 kcal mol^{-1}. Even when an E_b value of only 15 kcal mol^{-1} is taken and an $RO_2 + NO \rightarrow RO + NO_2$ exoergicity of 12 kcal mol^{-1} is assumed, the theoretically calculated prompt dissociation fraction is negligibly small (<2%), in agreement with the experimental findings. An upper limit to the decomposition rate of 100 s^{-1} can be obtained from our estimate of $k_{18}/k_{19} = (6 \pm 3) \times 10^{15}$ molecule cm^{-3}, assuming that the rate coefficient for reaction 19 is similar to that for the reaction of ethoxy with O_2. If the A factor for decomposition is similar to that in reaction 6, an estimate of the barrier height of 15−16 kcal mol^{-1} is obtained, in accord with the experimental and theoretical findings. Thus, we conclude that the major difference in the behavior of the β-hydroxy- and β-chloroalkoxy radicals can be attributed to the difference in the barrier heights to dissociation associated with the higher ionization potential of the leaving group.

Atmospheric Implications. As in previous studies,[12−14] the OH-initiated oxidation of ethene has been shown to yield CH_2O and glycolaldehyde as the major products. However, we have shown that the mechanism is more complicated than previously assumed and occurs via the production of a chemically activated oxy radical, $HOCH_2CH_2O^*$. This mechanism must be taken into account to understand the products obtained in the oxidation of ethene in different regions of the atmosphere. In urban and rural regions, the chemistry of the peroxy radical will be dominated by its reaction with NO, reaction 3, and yields of formaldehyde (1.6 molecules produced per ethene consumed) and glycolaldehyde (0.2 molecules produced per ethene con-

sumed) are the same as those reported by Niki et al.[13] In the upper troposphere, NO levels are again sufficiently high to control the RO_2 reactivity and prompt decomposition of the excited RO radicals will give a formaldehyde yield of about 0.5 molecules per ethene consumed. The remainder of the radicals will be thermalized and react essentially exclusively with O_2 at the low temperatures present there, giving a glycolaldehyde yield of about 0.75. In the cleaner regions of the free troposphere and in the marine boundary layer, where NO_x concentrations are low, other reactions of the peroxy radicals will occur (i.e., reaction with HO_2 and possibly CH_3O_2 and other peroxy radicals), and the fate of ethene in these regions will have to be determined by chemical models.

The oxidation of ethene by chlorine atoms is probably only of significance in the marine boundary layer, particularly during Arctic sunrise,[47] where evidence for elevated Cl atom concentrations have been reported.[48] The dominant fate of the $ClCH_2CH_2O$ radical produced in the Cl-initiated oxidation of ethene will be reaction with O_2 to produce $ClCH_2CHO$.

Conclusions

The OH-initiated oxidation of ethene has been shown to yield formaldehyde and glycolaldehyde as major products. The oxidation in the presence of NO_x has been shown to occur via the formation of an excited oxy radical, $HOCH_2CH_2O^*$. About 25% of these excited radicals decompose promptly to yield formaldehyde, while the remainder are thermalized and undergo competition between reaction 6 and reaction 7. The rate coefficient ratio k_6/k_7 has been determined to be $(2.0 \times 10^{25}) \exp(-4200/T)$ molecule cm^{-3} over the temperature range 250−325 K. The results are in good quantitative agreement with calculations of the decomposition rates of both chemically activated and thermalized oxy radicals. Of controlling importance to these decomposition rates is that the intramolecular H-bonding stabilization by about 2 kcal mol^{-1} persists in the transition state, notwithstanding the greatly increased C−C bond length.[38] The yield of formaldehyde in the oxidation of ethene in the troposphere will be a strong function of temperature and will range from a maximum value of 1.6 near the Earth's surface to a low value of 0.5 in the upper troposphere. In contrast, the chlorine initiated oxidation of ethene does not lead to C−C bond scission, even in the presence of NO.

Acknowledgment. This work was funded by the Upper Atmosphere Research Program of the NASA Mission to Planet Earth. NCAR is sponsored by the National Science Foundation. L.V. and J.P. are indebted to the European Commission for financial support. Thanks are due to Frank Flocke of NCAR for his help in the preparation of the methyl nitrite sample and to Chris Cantrell and Laura Iraci for helpful comments on the manuscript.

References and Notes

(1) Sawada, S.; Totsuka, T. *Atmos. Environ.* **1986,** *20*, 821.

(2) Singh, H. B.; Zimmerman, P. R. Atmospheric distribution and sources of nonmethane hydrocarbons. In *Gaseous Pollutants: Characterization and Cycling;* Nriagu, J. O., Ed.; John Wiley: New York, 1992; pp 177−235.

(3) Greenberg, J. P.; Zimmerman, P. R. *J. Geophys. Res.* **1984**, *89*, 4767.

(4) Rudolph, J. *J. Geophys. Res.* **1988**, *93*, 8367.

(5) Blake, N. J.; Blake, D. R.; Sive, B. C.; Chen, T.-Y.; Rowland, F. S.; Collins, J. E., Jr.; Sachse, G. S.; Anderson, B. E. *J. Geophys. Res.* **1996**, *101*, 24151.

(6) Singh, H. B.; Herlth, D.; Kolyer, R.; Chatfield, R.; Viezee, W.; Salas, L. J.; Chen, Y.; Bradshaw, J. D.; Sandholm, S. T.; Talbot, R.; Gregory, G. L.; Anderson, B.; Sachse, G. W.; Browell, E.; Bachmeier, A. S.; Blake, D. R.; Heikes, B.; Jacob, D.; Fuelberg, H. E. *J. Geophys. Res.* **1996**, *101*, 24203.

(7) Atkinson, R. *J. Phys. Chem. Ref. Data* **1997**, *26*, 215.

(8) DeMore, W. B.; Sander, S. P.; Golden, D. M.; Hampson, R. F.; Kurylo, M. J.; Howard, C J.; Ravishankara, A. R.; Kolb, C. E.; Molina, M. J. *Chemical kinetics and photochemical data for use in stratospheric modeling; evaluation number 12*; NASA JPL Publ. No. 97-4; 1997.

(9) Miyoshi, A.; Matsui, H.; Washida, N. *Chem. Phys. Lett.* **1989**, *160*, 291.

(10) Murrells, T. P.; Jenkin, M. E.; Shalliker, S. J.; Hayman, G. D. *J. Chem. Soc., Faraday Trans.* **1991**, *87*, 2351.

(11) Becker, K. H.; Geiger, H.; Wiesen, P. *Chem. Phys. Lett.* **1991**, *184*, 256.

(12) Niki, H.; Maker, P. D.; Savage, C. M.; Breitenbach, L. P. *J. Phys. Chem.* **1978**, *82*, 135.

(13) Niki, H.; Maker, P. D.; Savage, C. M.; Breitenbach, L. P. *Chem. Phys. Lett.* **1981**, *80*, 499.

(14) Barnes, I.; Becker, K. H.; Ruppert, L. *Chem. Phys. Lett.* **1993**, *203*, 295.

(15) Atkinson, R.; Carter, W. P. L. *J. Atmos. Chem.* **1991**, *13*, 195.

(16) Atkinson, R. *Int. J. Chem. Kinet.* **1997**, *29*, 99.

(17) Wallington, T. J.; Hurley, M. D.; Fracheboud, J. M.; Orlando, J. J.; Tyndall, G. S.; Sehested, J.; Møgelberg, T. E.; Nielsen, O. J. *J. Phys. Chem.* **1996**, *100*, 18116.

(18) Møgelberg, T. E.; Sehested, J.; Tyndall, G. S.; Orlando, J. J.; Fracheboud, J.-M.; Wallington, T. J. *J. Phys. Chem. A* **1997**, *101*, 2828.

(19) Bilde, M.; Wallington, T. J.; Ferronato, C.; Orlando, J. J.; Tyndall, G. S.; Estupiñan, E.; Haberkorn, S. *J. Phys. Chem. A* **1998**, *102*, 1976.

(20) Shetter, R. E.; Davidson, J. A.; Cantrell, C. A.; Calvert, J. G. *Rev. Sci. Instrum.* **1987**, *58*, 1427.

(21) Tyndall, G. S.; Orlando, J. J.; Calvert, J. G. *Environ. Sci. Technol.* **1995**, *28*, 202.

(22) Taylor, W. D.; Allston, T. D.; Moscato, M. J.; Fazekas, G. B.; Kozlowski, R.; Takacs, G. A. *Int. J. Chem. Kinet.* **1980**, *12*, 231.

(23) Wallington, T. J.; Andino, J. M.; Lorkovic, I. M.; Kaiser, E. W.; Marston, G. *J. Phys. Chem.* **1990**, *94*, 3644.

(24) Niki, H.; Maker, P. D.; Savage, C. M.; Hurley, M. D. *J. Phys. Chem.* **1987**, *91*, 2174.

(25) Yarwood, G.; Peng, N.; Niki, H. *Int. J. Chem. Kinet.* **1992**, *24*, 369.

(26) Atkinson, R.; Baulch, D. L.; Cox, R. A.; Hampson, R. F., Jr.; Kerr, J. A.; Troe, J. *J. Phys. Chem. Ref. Data* **1992**, *21*, 1125.

(27) Wallington, T. J.; Andino, J. M.; Japar, S. M. *Chem. Phys. Lett.* **1990**, *165*, 189.

(28) Kaiser, E. W.; Wallington, T. J. *J. Phys. Chem.* **1994**, *98*, 5679.

(29) Wallington, T. J.; Orlando, J. J.; Tyndall, G. S. *J. Phys. Chem.* **1995**, *99*, 9437.

(30) Braun, W.; Herron, J. T.; Kahaner, D. K. *Int. J. Chem. Kinet.* **1988**, *20*, 51.

(31) Catoire, V.; Lesclaux, R.; Lightfoot, P. D.; Rayez, M.-T. *J. Phys. Chem.* **1994**, *98*, 2889.

(32) Staffelbach, T. A.; Orlando, J. J.; Tyndall, G. S.; Calvert, J. G. *J. Geophys. Res.* **1995**, *100*, 14189.

(33) Barnes, I.; Bastian, V.; Becker, K. H.; Overath, R.; Tong, Z. *Int. J. Chem. Kinet.* **1989**, *21*, 499.

(34) Jungkamp, T. P. W.; Smith, J. N.; Seinfeld, J. H. *J. Phys. Chem. A* **1997**, *101*, 4392.

(35) Wittig, C.; Nadler, I.; Reisler, H.; Noble, M.; Catanzarite, J.; Radhakrishnan, G. *J. Chem. Phys.* **1985**, *83*, 5581.

(36) Nesbitt, D. J.; Petek, H.; Foltz, M. F.; Filseth, S. V.; Bamford, D. J.; Moore, C. B. *J. Chem. Phys.* **1985**, *83*, 223.

(37) Stein, S. E.; Rabinovitch, B. S. *J. Chem. Phys.* **1973**, *58*, 2438.

(38) Vereecken, L.; Peeters, J. Theoretical investigation of the role of intramolecular hydrogen bonding in β-hydroxyethoxy and β-hydroxyethylperoxy radicals. *J. Phys. Chem. A*, submitted.

(39) Forst, W. *Theory of Unimolecular Reactions*; Academic Press: New York, 1973.

(40) Vereecken, L.; Huyberechts, G.; Peeters, J. *J. Chem. Phys.* **1997**, *106*, 6564.

(41) Gillespie, D. T. *J. Phys. Chem.* **1977**, *81*, 2340.

(42) Oref, I.; Tardy, D. C. *Chem. Rev.* **1990**, *90*, 1407.

(43) Vereecken, L.; Pierloot, K.; Peeters, J. *J. Chem. Phys.* **1998**, *108*, 1068.

(44) Troe, J. *J. Chem. Phys.* **1977**, *66*, 4758.

(45) Troe, J. *J. Chem. Phys.* **1979**, *83*, 114.

(46) Lias, S. G.; Bartmess, J. E.; Liebman, J. F.; Holmes, J. L.; Levin, R. D.; Mallard, W. G. *J. Phys. Chem. Ref. Data* **1988**, *17*, 1.

(47) Barrie, L. A.; Bottenheim, J. W.; Hart, W. R. *J. Geophys. Res.* **1994**, *99*, 25313.

(48) Jobson, B. T.; Niki, H.; Yokouchi, Y.; Bottenheim, J.; Hopper, F.; Leaitch, R. *J. Geophys. Res.* **1994**, *99*, 25355.